Electrical Power and Energy Systems 84 (2017) 87–98

Contents lists available at ScienceDirect

Electrical Power and Energy Systems

journal homepage: www.elsevier.com/locate/ijepes

Active–reactive power approaches for optimal placement of charge stations in power systems

Cheng Wang, Roderick Dunn, Francis Robinson, Bo Lian *, Weijia Yuan, Miles Redfern

Department of Electrical and Electronic Engineering, University of Bath, United Kingdom

ARTICLE INFO

Article history:
Received 29 September 2015
Received in revised form 12 April 2016
Accepted 13 April 2016

Keywords:
Charge stations' location
EVs
Active and reactive power optimisation
Power loss reduction

ABSTRACT

Electric Vehicles (EVs) have been suggested as alternatives to conventional vehicles for reducing petrol consumption and carbon dioxide (CO_2) emissions. When a large number of EVs connect to the grid, they can cause a large amount of power loss. Where to install multiple charge stations in the grid, so as to mitigate losses caused by EVs when providing energy to those EVs, is becoming vitally important. In this paper, a distribution test-network model is described. A new analytical method is proposed, using the stations' cooperation in terms of optimal active and reactive power dispatch as well as power flow analysis for locating the optimal placement of charge stations, so as to reduce power losses. This method is compared with the previously developed current density method for single charge stations using system simulation results. It was demonstrated that the methods proposed in this paper are more accurate than the current density method, and that 17% of the average active power loss can be saved for three different types of load profile. In addition, 27% of the average active power loss was saved by installing two charge stations rather than no charge stations in the test-line. It is shown that this could represent a 2.6% annual yield above inflation for investing in installing and running such charge stations.

Introduction

In order to reduce CO_2 emissions, more attention is being paid to Electric Vehicles (EV) than before. However, the driving range limitation is still a big concern for all EV drivers. This problem can be solved either by improving the state-of-the-art of EV batteries or by building charge stations into Distribution Networks (DN) and Transmission Networks (TN) [1,2].

The state-of-the-art of batteries is restricted by material science and physics. The charge station is a relatively mature technology and with an increasing number of EVs will become an essential part of the commercial chain. In Ref. [3] the researchers concentrated on designing multi-charge stations for vehicles together with their utilization in the grid by considering battery replacement, charging and vehicle to grid. In Refs. [4,5] the authors considered both EV arrival time, departure time, energy demands, and real world parking statistics. Based on these data the papers provided charge station scheduling strategies. Refs. [6–8] concentrated more on the optimal planning and economic aspects of a charge station for EV; by considering various costs, to achieve comprehensive cost and energy loss minimisation. As an alternative, Refs. [9,10] focused on optimisation of EV charge station location; by using the conservation theory of regional traffic flows, taking EVs as fixed load points for the charge station. The maintenance and capital cost minimisation for a charge station was considered in this work.

In [11] the Battery Energy Storage System (BESS) was considered as a design criteria in charge stations. By using this criteria the EV charge efficiency and time was improved. In [12] the concept of combined photovoltaic systems and battery unit multi-supply systems was mentioned. In [13] the BESS was installed in fast charge stations as an energy supplier. The daily operating cost was minimised by optimising the active power of the BESS. Meanwhile, charging loads were smoothed and high-price electricity absorption from the grid was avoided.

The common drawback of these papers is that no matter what type of method were used to optimise the size and location, and to minimise the various costs of those stations, the energy transfer between charge stations was not considered. For example, combined BESSs in charge stations can store off-peak energy and use it to provide energy to EVs during peak-time. But these charge stations do not provide energy to each other. In this paper cooperation between two charge stations, in terms of transferring energy to each other, is specified and tested for four different operation scenarios. This cooperation makes charge stations able to support each other, reduce losses further and provide energy to customers.

* Corresponding author.

http://dx.doi.org/10.1016/j.ijepes.2016.04.047
0142-0615/

Nomenclature

T	life time of charge station 15 year
$C_{pi}^{on}(t)$	peak electricity price \$0.068/kW h
C_{pi}^{off}	off-peak electricity price \$0.014/kW h
T_{CHi}	annual utilization hours of charging devices 8 h/ per-day
$C_{ETi}^{I}(t)$	per-unit investment cost of transformers \$40.84/kV A
$C_{CHi}^{I}(t)$	per-unit investment cost of charging devices \$34.71/ KVA
C_{DEi}^{I}	per-unit investment cost of other devices \$30.94/KVA
$C_{EAi}^{I}(t)$	land utilization cost \$95.63/m^2
C_{Bsi}^{I}	per-unit investment cost of battery \$5.21/kV A
$\boldsymbol{C_{VCi}^{O}(t)}$	active, reactive power filtering and compensation cost \$10.16/kV A
$C_{HRi}(t)$	human resources cost \$16476.41
$C_{Bsi}^{OM}(t)$	per-unit operation and maintain cost of battery \$2500/ MW
$C_{ETi}^{M}(t)$	per-unit maintenance cost of transformers \$11.92/kV A
$C_{CHi}^{M}(t)$	per-unit maintenance cost of charging devices \$8.92/ kV A
C_{DEi}^{M}	per-unit maintenance cost other devices \$100/kW h
$\eta CHij$	charging efficiency of charge devices 90%
$\cos\emptyset CHij$	power factor of charge devices 0.95
K_i	simultaneity coefficient 0.8
n_i	the number of charging devices 10
i	the discount rate 10%
E_i	battery charging efficiency 90%
H_{aver}	the average EVs charging time 4 h

Installing combined BESS charge stations brings some additional problems, one of which is where to install these charge stations in the power system. In existing literature the optimal location problem has been treated in the following ways. In [14] the author proposed a maximisation of the wind energy method based on Ontario's standard offer program for locating a BESS in a DN with high penetration of wind energy. In [15] the author used a hybrid Genetic Algorithm (GA) combined with quadratic programming to size and site the BESS, so as to reduce network losses and cost. In [16] a hybrid method relying on dynamic programming with a GA was described. Through this method the location, rating and control strategy of the BESS were found, and overall investments and network costs were minimised. A methodology proposed in [17] was to optimise the location of the BESS in DNs and also to mitigate problems created by high penetration of renewable Distribution Generation (DG). A two segment current density integration method was used in [18] for choosing the optimal location of DG in a single-DG system. The method was tested and proved using an 11-bus distribution line network.

However, these methods did not consider the active and reactive power transferring between two BESSs when choosing the location. The research described by the authors of this paper expands on the current density integration method for a two charge station system. The new method identifies the optimal location for the second charge station given the optimal location of the first charge station. The developed method was tested in the same system as [18] using four different operational scenarios. It was found that the current density method was accurate for the system with one charge station, but it could not be applied to a system that had two charge stations, under several different operational scenarios, because it only considered one current component from the BESSs. Therefore, an analytical cooperation approach, combining active and reactive power optimisation methods, was proposed to address this. This method was more accurate than the current density method. The results were compared with the current density method not only as a mathematical model, but also considering the cost of power loss.

After finding the locations of charge stations, the costs and profits of the charge stations were analysed. From the results, the owners of the charge stations can earn 0.84 million dollars over 15 years'. Further benefits, for example by providing voltage support and load peak shaving services to the DN could be obtained from operation.

The rest of this paper is structured as follows: In Section 'System modelling' system modelling is introduced and an BESS model is built. Section 'Theoretical analysis' provides a theoretical analysis of the optimal placement of a charge station for power loss reduction and a costs and profits analysis. In this section a current density integration method and the analytical method, combined with a π line model, are presented. In Section 'Simulation results and discussions' the old [18] and new methods' results are compared and analysed. Both methods are used with the 11-bus test-line used in [18]. Based on that test-line, four different operation scenarios were used. These cover normal working conditions (scenario one and four) and energy cooperation conditions (scenario two and three) for two charge stations, identifying the optimal location for the charge stations. Section 'Conclusion' gives the outcomes and conclusions of the research.

System modelling

System load modelling

In order to test the proposed method three load periods, two off-peak (00:30–05:30 h and 05:30–20:30 h) and one peak (20:30–23:30 h), for a typical day [19] were chosen to separate each 24 h into three power demand periods. These can be seen in Fig. 1. The 11-bus distribution test-line with three different types of load profile, which can illustrate the majority of load patterns in such power systems, was used in this paper for identifying the optimal location of the charge stations [18].

It can be seen from Fig. 1 that during the first and second off-peak periods the BESS can store energy from the TN, This energy can be purchased at a low price, whereas during the on-peak period the BESS can dispatch the stored energy to customers. This will not only save money on their electricity bill, but also enhance system stability [20].

Specifications and modelling of EVs

According to recent EV market surveys [21–23], the Chevrolet Volt plug-in hybrid occupied 41% of the whole electric vehicle market, the Nissan Leaf all-electric car accounted for 30%, the Toyota Prius Plug-in Hybrid took up 17%, while the Tesla Model S had the remaining 12% of the market. Therefore, an assumption was made that, for a mid-sized city there are 100 EV owners [24], 41 used Chevrolet Volt Plug-in Hybrid cars, 30 used Nissan Leaf all-electric cars, 17 used Toyota Prius Plug-in Hybrid cars, and 12 used the Tesla Model S. The characteristics of the different electric vehicles are shown in Table 1 [25].

Level 1 Charging is the slowest level. It provides a single phase 120 V/15 A AC plug. This type of charge is suitable for the home

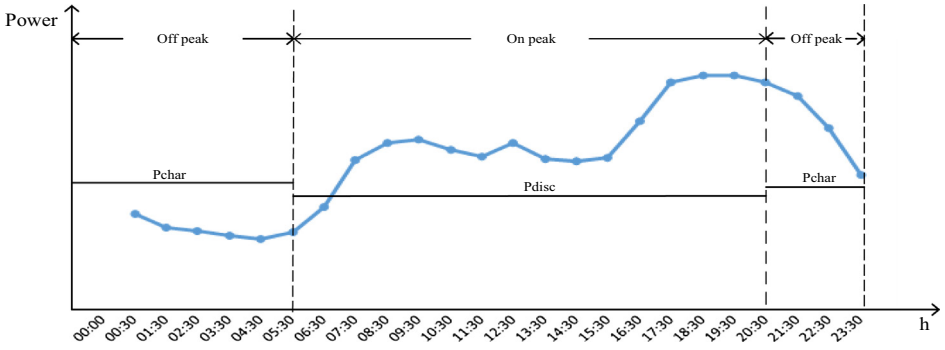

Fig. 1. Three periods of daily electricity demand [15].

Table 1
Characteristic of the EV.

EV types	Level 1 Charge		Level 2 Charge		DC Fast	
	Power demand	Time	PD	Time	PD	Time
Chevrolet Volt	0.96–1.4 kW	5–8 h	3.8 kW	2 h	n/a	n/a
Nissan Leaf	1.8 kW	12–16 h	3.3 kW	7 h	50+ kW	15–30 m
Prius	1.4 kW (120 V)	3 h	3.8 kW (240 V)	2.5 h	n/a	n/a
Tesla Model S	1.8 kW	30+ h	16.8 kW	4 h	n/a	n/a

charge during the night, no additional infrastructure is necessary [25].

Level 2 Charging is the primary option for a public or commercial charge station. This charge option can operate at up to 80 A and 19.2 kW. This charging is not suitable for home and private use, but is suitable for public charging [26].

DC Fast Charging is much faster than other methods. It can be installed in charge stations, but usually requires a 480 V AC input [26] and power electronics to convert AC to DC.

In this research Level 2 Charging was chosen. The charge time was chosen as the average charge time of the four types of EV, which was four hours.

The power demand of each type of EV in one timeslot can be calculated by using Eq. (1) [27].

$$P_i(t) = \frac{[b_i - x_i(t)] \times C_i}{E_i H_{aver}}, \quad \forall i, t \tag{1}$$

where $P_i(t)$ is the power demand of the EV at any timeslot t. b_i is the desired State of Charge (SOC). $x_i(t)$ is the SOC at the beginning of t. C_i is the capacity of the EV. E_i is the battery charging efficiency of the EV, H_{aver} is the EV's average charge time.

The total power demand of all EVs can be express as shown in Eq. (2).

$$P_T(t) = \sum_{i=1}^{41} P_{i(t)c} + \sum_{i=1}^{30} P_{i(t)n} + \sum_{i=1}^{17} P_{i(t)p} + \sum_{i=1}^{12} P_{i(t)t} \tag{2}$$

where $P_T(t)$ are the total power demands of all types of EVs. $P_{i(t)c}, P_{i(t)n}, P_{i(t)p}$, and P_{itt} are the power demand for each type, i.e. Chevrolet, Nissan Leaf, Prius, and Tesla.

These EVs were added into the test-line at the locations seen in Fig. 2.

The modelling of combined BESS charge station

The combined BESS charge station is different compare with the traditional charge station. Traditional stations are not able to store off-peak energy and sell it to EVs and local residents at any time. Whereas, BESS can make the profits by utilising electricity price differences between peak and off-peak times. The configuration of the stations can be seen in Fig. 3.

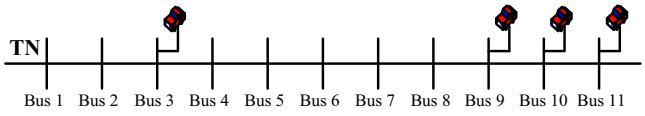

Fig. 2. A test-line with EVs.

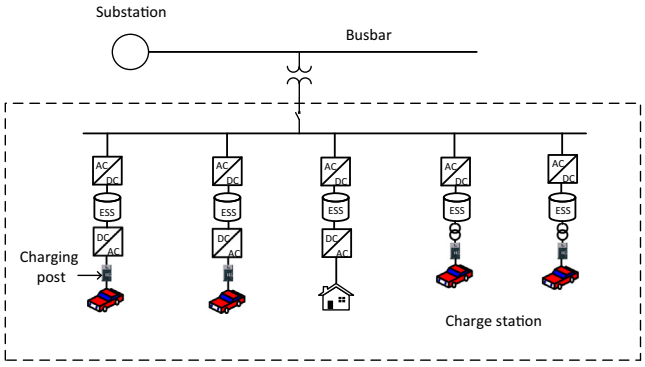

Fig. 3. Charge station's configuration.

The charge station consists of BESSs, normal charging points and relevant charging facilities such as transformers, active and reactive compensators, inverters and converters, and charging spaces.

The BESS consists of batteries and Power Conditioning Systems (PCS) [20,28].

A simple PCS consists of electronic devices such as capacitors, diodes and transformers, the structure can be seen in Fig. 4. The PCS capability is show in Fig. 5. At operation point 1 active and reactive power is being discharged to the system. At operation point 2 the system is being charged, absorbing both active and reactive power from the TN [29]. Based on the independent and

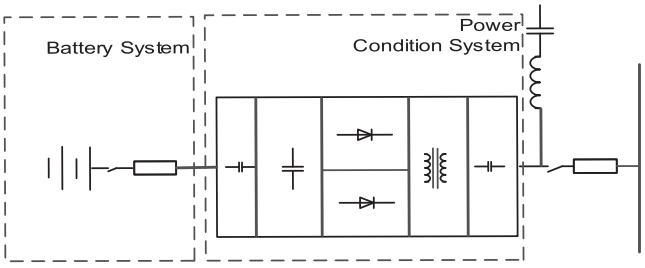

Fig. 4. The structure of BESS.

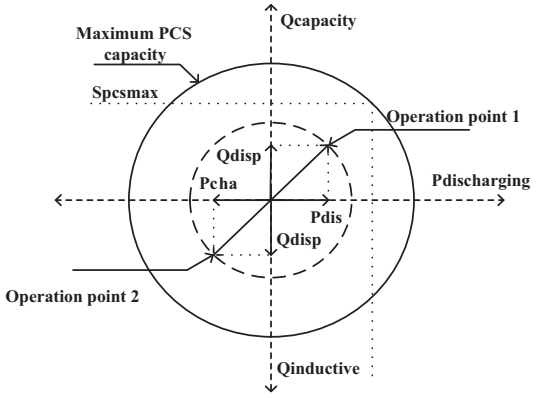

Fig. 5. Active and reactive power capability [29].

rapid control capability of the PCS, active discharge and reactive power dispatch were set as controlled variables when identifying charge station two's optimal location. It is noted that active power can be either charging or discharging at any given time.

The active and reactive power discharge of BESS should not exceed the maximum apparent power $S_{BESSmax}$ of the BESS [30].

$$P_{dis}^2 + Q_{dis}^2 \leqslant S_{BESSmax}^2 \tag{3}$$

$$P_{char}^2 + Q_{disc}^2 \leqslant S_{BESSmax}^2 \tag{4}$$

The active power for charging and discharging must be positive values

$$P_{char(k,h)} \geqslant 0, \quad P_{dis(k,h)} \geqslant 0 \tag{5}$$

$$-S_{ESSmax(k,h)}^2 \leqslant Q_{dis(k,h)} \tag{6}$$

Moreover the upper and lower bound of the storage capacity should satisfy.

$$E_{min} \leqslant E_{Low}, \quad E_{Up} \leqslant E_{max} \tag{7}$$

The EV's impact modelling and four operation scenarios

For the sake of modelling the EV's impact in terms of active and reactive power losses, and observing the power losses for the test-line without a charge station, with one charge station and with two charge stations, power flow analysis was used.

Four different operation scenarios, in terms of the cooperation between two charge stations, are listed below. The first scenario is for normal EV charge requirements, where a regular amount of drivers charge their EVs at the charge station. The second and the third scenario are designed for some exceptional events, where one charge station runs out of energy and needs to borrow it from other sources. The last scenario is where the EV's energy requirements exceed both charge stations' designed capacity; this time both stations need external energy from the TN.

(1) The first scenario is the most common one, both charge stations used their full charged capacity to charge EVs without any optimised power charge and discharge.
(2) The second scenario considers both charge and discharge processes as charge station two runs out of rated energy. Charge station one needs to transfer energy to charge station two. The active and reactive discharge power from station one will be optimised.
(3) The third scenario also considers both charge and discharge processes, but here charge station one runs out of rated energy. Charge station two needs to transfer energy to charge station one. The active discharge and reactive dispatch power from station two will be optimised.
(4) The fourth scenario is where both charge stations one and two cannot supply the EVs and loads. External energy from the TN is used to charge stations one and two. The active and reactive power from the TN will be optimised to charge both stations. Tables 2–4 show comparisons of active and reactive power losses without charge stations, with one charge station and with two charge stations in 11-bus distribution test-line.

Theoretical analysis

The main focus of this paper is to identify charge station two's optimal location. In practice, there are many additional constrains for the optimisation of charge station's location, such as different countries' energy policies and geographic factors. This paper does not consider these factors.

Analytical approach for optimal location

In order to reduce the power loss caused by EV penetration, a distribution network with charge stations one and two, which are S_1 and S_2 are shown in Fig. 6, and the π line model [31] was created and developed for analysing the location of station two for loss reduction. The active, reactive power flow, bus voltage and current of π line model are given by Eqs. (8)–(14).

P_i and Q_i are the sending-end active and reactive power through bus S_1 and S_2

$$P_i = P_i' + R_i \frac{P_i'^2 + Q_i'^2}{V_{s2}^2} \tag{8}$$

$$Q_i = Q_i'' - V_{s1}^2 \frac{Yi}{2} = Q_i' + X_i \frac{P_i'^2 + Q_i'^2}{V_{s2}^2} - V_{s1}^2 \frac{Yi}{2} \tag{9}$$

P_i' and Q_i' are the injection active power and reactive power to bus S_2 respectively

$$P_i' = P_{dis2} + P_{load2} + P_{m2F} - P_{grid} - P_{dis1} \tag{10}$$

$$Q_i' = Q_{dis2} + Q_{load2} + Q_{m2F} - Q_{grid} - Q_{dis1} - V_{s2}^2 \frac{Yi}{2} \tag{11}$$

The voltage at bus S_2 is

$$V_{s2} = V_{s1} - I_i Z_i = V_{s1} - \frac{S_i''^*}{V_{s1}^*}(R_i + jX_i) \tag{12}$$

$$\begin{aligned} V_{s2} &= V_{s1} - \frac{P_i'' - jQ_i''}{V_{s1}}(R_i + jX_i) \\ &= \left(V_{s1} - \frac{P_i'' R_i + Q_i'' X_i}{V_{s1}}\right) - j\left(\frac{P_i'' X_i - Q_i'' R_i}{V_{s1}}\right) \end{aligned} \tag{13}$$

The current through the π line model is

Table 2
First scenario comparison of power loss.

First scenario	Without stations		Charge station one		Both charge stations	
	P_{loss}	Q_{loss}	P_{loss}	Q_{loss}	P_{loss}	Q_{loss}
Uniform	0.682	0.59	0.616	0.53	0.190	0.25
Central	0.251	0.22	0.215	0.18	0.058	0.06
Increasing	0.565	0.49	0.532	0.46	0.171	0.21

Table 3
Second scenario comparison of power loss.

Second scenario	Without stations		Charge station one		Both charge stations	
	P_{loss}	Q_{loss}	P_{loss}	Q_{loss}	P_{loss}	Q_{loss}
Uniform	0.682	0.59	0.801	0.69	0.596	0.51
Central	0.251	0.22	0.319	0.27	0.215	0.18
Increasing	0.565	0.49	0.655	0.56	0.387	0.33

Table 4
Third scenario comparison of power loss.

Third scenario	Without stations		Charge station one		Both charge stations	
	P_{loss}	Q_{loss}	P_{loss}	Q_{loss}	P_{loss}	Q_{loss}
Uniform	0.682	0.59	0.741	0.64	0.136	0.14
Central	0.251	0.22	0.284	0.24	0.093	0.08
Increasing	0.565	0.49	0.609	0.52	0.094	0.08

$$I_i = \sqrt{\frac{P_i^2 + Q_i^2}{V_{s1}^2}} \tag{14}$$

The series impedance and shunt admittance between bus S_1 and S_2, are $(R_i + jX_i)$ and $Yi/2$ respectively. P_i' and Q_i' are the injection active power and reactive power to bus S_2 respectively. P_{dis} and Q_{dis} are the active and reactive discharge power of station.

Where $S_i'' = P_i'' + Q_i''$, $P_i'' = P_i$, $Q_i'' = Q_i + V_{s1}^2 \frac{Yi}{2}$. P_{grid} and the Q_{grid} are the active and reactive power injected by the TN. P_{load1}, P_{load2}, Q_{load1}, and Q_{load2} are the total active and reactive power load at bus S_1 and S_2. P_{m1F}, P_{m2F}, Q_{m1F} and Q_{m2F}, are the sum of active and reactive power flows through all downstream branches connected to buses S_1 and S_2.

To find the optimal location of charge station two, an objective function was built and can be seen from Eq. (16).

$$f_j = \sum_{i=1}^{j} R_{1i(j)} \left| P_i' + jQ_i' \right|^2 \quad j = 3, 4, 5 \cdots N \tag{15}$$

The goal is to find the optimal location for charge station two, where Eq. (16) reaches the minimum value.

$$F_m = Min\, f_j \tag{16}$$

The $R_{1i(j)}$ is the resistance between two charge stations. N is the test system's total bus number. P_{load2} is the load at bus S_2. P_{m2F} is active power injection from bus S_2. P_{dis1} and P_{dis2} can be obtained from Eq. (17) by using the MATLAB optimisation programming.

$$Min\ P_L = \sum_{\forall s_1, s_2}^{s_1, s_2 \in S_B} I_i^2 R_i = \sum_{\forall s_1, s_2}^{s_1, s_2 \in S_B} \left(\frac{P_i^2 + Q_i^2}{V_{s_1}^2} \right) R_i \tag{17}$$

Both Eqs. (16) and (17) must satisfy the constraints, based on equations in (3)–(7), (18)–(23).

The active and reactive power flow in π line model must satisfy Eqs. (18) and (19).

$$P_i - P_i' - R_i \frac{P_i'^2 + Q_i'^2}{V_{s2}^2} = 0 \tag{18}$$

$$Q_i - Q_i' - X_i \frac{P_i'^2 + Q_i'^2}{V_{s2}^2} + V_{s1}^2 \frac{Yi}{2} = 0 \tag{19}$$

The voltage magnitudes at the sending bus and receiving bus must satisfy Eq. (20).

$$V_{s2}^2 - \left\{ V_{s1}^2 - 2\left(P_i'' R_i + Q_i'' X_i\right) + \frac{\left(P_i''^2 + Q_i''^2\right)\left(R_i^2 + X_i^2\right)}{V_{s1}} \right\} = 0 \tag{20}$$

The line current of the π line model should be within the thermal limit

$$I_i \leqslant I_i^{rated} \tag{21}$$

The bus voltages should not exceed the maximum and below the minimum voltage

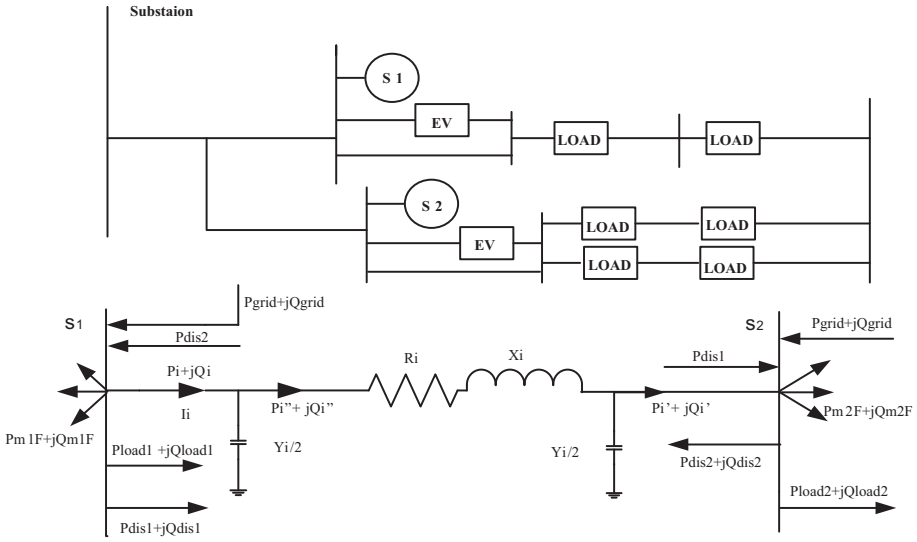

Fig. 6. Power flow analysis.

$$V_{s1}^{min} \leqslant V_{s1} \leqslant V_{s1}^{max} \tag{22}$$

$$V_{s2}^{min} \leqslant V_{s2} \leqslant V_{s2}^{max} \tag{23}$$

The theoretical procedures to find the optimal bus to locate station two are summarised below:

(1) Add EVs randomly into the 11-bus test-line.
(2) Run simulations and use power flow analysis to find the largest power loss bus and install charge station one there.
(3) Use the π line model in Fig. 6 to analyse the power loss between S_1 and S_2, which can be seen from Eqs. (8)–(17).
(4) Set $P_{dis1}, P_{dis2}, Q_{dis1}, Q_{dis2}$, as the variables for power losses minimisation.
(5) Use MATLAB optimisation programming to obtain these variables' values from Eq. (17).
(6) Use these values as the input values for objective function 16 and get values of each bus.
(7) Compare the objective function's values with the simulation results.

The current density method for optimal location

In previous research the phase current density method was used for analysis of power losses and identifying a DG's optimal location in a one DG system [18]. In this paper phase current I_i density was used for the same purpose, but different power cooperation strategies, between charge station one and two, were considered.

Using the current density method, the phasor feeder current at point x is

$$I(x, T_i) = \int_0^x I_d(x, T_i)dx \tag{24}$$

The incremental power loss at point x is

$$dP(x, T_i) = \left(\left|\int_0^x I_d(x, T_i)dx\right|\right)^2 \cdot Rdx \tag{25}$$

The total power loss along the feeder within the time duration T_i is

$$P_{loss}(T_i) = \int_0^l dP(x, T_i) = \int_0^l \left(\int_0^x I_i(x, T_i)dx\right)^2 \cdot Rdx \tag{26}$$

Firstly, it is considered that there is only one charge station in the test distribution line at location x_0 shown in Fig. 7. As a result of charge station two being added into the distribution line, two parameters (load current density $I_d(x, T_i)$ and load current) are changed in terms of current. The load current density will decrease, caused by voltage improvements due to adding station two, this decrease causes the feeder current to decrease. Meanwhile, with station two's current injection, the feeder current between the TN at l and the location of station two at x_0 will also change. But, compared with the change of load current density, the change of injected current from station two is influenced more by the change in feeder current. Hence, the change of load current density, caused by adding charge station two is neglected in this paper [18]. Therefore, the feeder current after adding station two can be obtained by using the load current density $I_d(x, T_i)$.

Secondly, consider the second charge station which is station one adds into test-line similarly. The change in the feeder current caused by injected current from station one is much higher than the change in the load current density. Therefore, the feeder current $I(x, T_i)$ can be expressed by using the $I_d(x, T_i)$ after two adding the charge station one and two. It can be seen from Eq. (27).

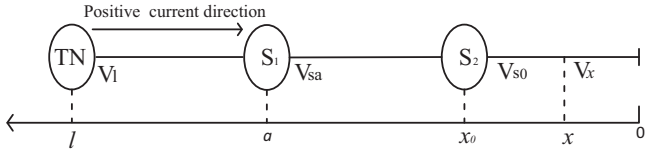

Fig. 7. A test-line with distributed load.

The feeder current $I(x, T_i)$ through that test line can be expressed as:

$$I(x, T_i) = \begin{cases} \int_0^x I_d(x, T_i)dx & 0 \leqslant x \leqslant x_0 \\ \int_0^x I_d(x, T_i)dx - I_{disc2} & x_0 \leqslant x \leqslant a \\ \int_0^x I_d(x, T_i)dx - I_{disc1} & a \leqslant x \leqslant l \end{cases} \tag{27}$$

The corresponding power loss in the feeder is

$$\begin{aligned} P_{loss}(x_0, T_i) = &\int_0^{x_0} \left(\left|\int_0^x I_d(x, T_i)dx\right|\right)^2 Rd_x \\ &+ \int_{x_0}^{a} \left(\left|\int_0^x I_d(x, T_i)dx - I_{disc2}\right|\right)^2 Rd_x \\ &+ \int_{a}^{l} \left(\left|\int_0^x I_d(x, T_i)dx - I_{disc1}\right|\right)^2 Rd_x \end{aligned} \tag{28}$$

The average power loss in a given time period T is

$$\overline{P_{loss}}(x_0) = \frac{1}{T}\sum_{i=1}^{N_t} P_{loss}(x_0, T_i)T_i \tag{29}$$

where N_t is the number of time durations in the time period T.

The target to minimise total average power loss

$$Target = Min\ P_{loss}(T) \tag{30}$$

The solution x_0 of Eq. (31) will give Eq. (30) the optimal site for power loss minimising.

$$\frac{\overline{P_{loss}}(x_0)}{d_{x_0}} = 0 \tag{31}$$

Assuming that charge station two is located at point x_0 according to Eq. (28), the effective power loss of the test feeder is

$$P_{loss}(x_0, T_i) = A + B + C \tag{32}$$

$$A = \left[I_d^2(T_i) \cdot \left(R\frac{x_0^3}{3}\right)\right] \tag{33}$$

$$B = \left[I_d^2(T_i) \cdot R\frac{a^3 - x_0^3}{3} + I_{disc2}^2(T_i) \cdot R(a - x_0) + I_d(T_i)I_{disc2}(T_i)R\left(a^2 - x_0^2\right)\right] \tag{34}$$

$$C = \left[I_d^2(T_i) \cdot R\frac{l^3 - a^3}{3} + I_{disc1}^2(T_i) \cdot R(l - a) + I_d(T_i)I_{disc1}(T_i)R\left(l^2 - a^2\right)\right] \tag{35}$$

where $I_d(x, T_i) = \frac{I_{load}(x, T_i)}{l}$, I_{load} is the load current at the sending-end of the feeder.

According to (31) and from Eqs. (33)–(35), Eq. (31) can be deduced as below

$$I_d^2(T_i)Rx_0 - I_{dis2}^2(T_i) \cdot R - 2I_d(T_i)I_{dis2}(T_i)Rx_0 = 0 \tag{36}$$

x_0 is obtained as below:

$$x_0 = \frac{l \cdot \sum_{i=1}^{N_t} I_{dis2}^2(T_i)T_i}{2\sum_{i=1}^{N_t} I_{load}(T_i)I_{dis2}(T_i)T_i} \tag{37}$$

Assuming the bus voltage along the feeders are in acceptable range, x_0 can be approximated as below:

$$x_0 = \frac{l \cdot \sum_{i=1}^{N_t} P_{dis2}^2(T_i)T_i}{2\sum_{i=1}^{N_t} P_{load}(T_i)P_{dis2}(T_i)T_i} \tag{38}$$

The goal is achieved by considering the power cooperation between both charge stations and using Eq. (31) to identify the optimal location for station two. It is assured that the voltage along feeder are in acceptable range 1 ± 0.05 p.u. and the transferred power is under line thermal limit.

The solution of x_0 of gives the optimal location of station two for the minimising of power loss for the test-line. It is assured that the voltage and transferred power are within system limitations. The theoretical procedures to find the optimal location of charge station two are summarised as follows:

(1) Add EVs randomly into 11-bus test-line.
(2) Run power flow analysis, and find the largest power loss bus and install charge station one there for four different operation scenarios.
(3) Find the distributed load $I_d(x, T_i)$ along the feeder l.
(4) Express the feeder current by using three segment current density integration methods.
(5) Use Eqs. (27) and (31) to calculate the average power loss and identify the optimal location x_0 for charge station two.
(6) Compare the optimal location x_0 with the system simulation's location.

The annual profit of the charge station

In order to calculate the profit of charge station, the revenues and costs of the station are obtained.

(1) The profit of the charge station is in Eq. (39).

$$P_{EVCSi}(t) = \sum_{t=1}^{T} R_{EVCSi}^{T}(t) - \sum_{t=1}^{T} C_{EVCSi}^{T}(t) \tag{39}$$

where $P_{EVCSi}(t)$ is the annual profit of charge station, $R_{EVCSi}^{T}(t)$ is revenue of charge station and $C_{EVCSi}^{T}(t)$ is total cost of station, T is the life time of station.

$R_{EVCSi}^{T}(t)$ can be expressed in Eq. (40).

$$R_{EVCSi}^{T}(t) = \sum_{t=1}^{T} [C_{pi}^{on}(t)E_{EV}T_{CHi} + C_{pi}^{off}(t)E_{Re}T_{CHi}] \tag{40}$$

where $C_{pi}^{on}(t)$ is the peak electricity price, C_{pi}^{off} is the off-peak price. E_{EV} and E_{Re} are the energy demand of EVs and local residents. T_{CHi} is the annual utilization hours of charging devices.

(2) The cost of the charge station includes investment cost $C_{EVCSi}^{I}(t)$, operation cost $C_{EVCSi}^{O}(t)$, maintenance cost $C_{Evcsi}^{M}(t)$ the network loss cost [32] can be shown in Eq. (41).

$$C_{EVCSi}^{T}(t) = \sum_{t=1}^{T} [C_{EVCSi}^{I}(t) + C_{EVCSi}^{O}(t) + C_{Evcsi}^{M}(t)] \tag{41}$$

The investment cost of charge station can be expressed in Eq. (42).

$$C_{EVCSi}^{I}(t) = C_{ETi}^{I}(t)S_{ETi} + C_{CHi}^{I}(t)S_{CHi} + C_{DEi}^{I}(t)S_{DEi} + C_{EAi}^{I}(t)F_{EAi} + C_{Bsi}^{I}(t)\frac{E_B}{\eta CHij} \tag{42}$$

where $C_{ETi}^{I}, C_{CHi}^{I}, C_{DEi}^{I}$ and C_{Bsi}^{I} are the capacity per-unit investment cost of transformers, charging devices, other devices and batteries. C_{EAi}^{I} is the land utilization cost. S_{ETi} are the transformers' capacities. S_{CHi} is the total capacity of the charging devices (including chargers, charging points). S_{DEi} is the total capacity of other devices except transformers and charging devices (for example loads and lighting). F_{EAi} is the area of ith charge station. E_B is the capacity of battery. $\eta CHij$ is the charging efficiency.

$$S_{ETi} = \frac{(S_{CHi} + S_{DEi})}{L_{EVCSi}^{max}} \tag{43}$$

where L_{EVCSi}^{max} is the daily maximal load rate of the ith EV charging station.

S_{CHi} is the rated power

$$S_{CHi} = K_i \sum_{j=1}^{n_i} S_{CHi} = K_i \sum_{j=1}^{n_i} \left(P_{CHij/\eta CHij \cos \emptyset CHij}\right) \tag{44}$$

where n_i and K_i are the number and simultaneity coefficient of the charging devices in ith charge station. P_{CHij} is the output active power. $\cos \emptyset CHij$ is the power factor and $\eta CHij$ is the charging efficiency in charging station.

The operation cost of ith charge station can be expressed in Eq. (45), which include charging cost $C_{CHi}^{O}(t)$, power consumption cost $C_{EEi}^{O}(t)$, active power filtering and reactive power compensation cost $C_{VCi}^{O}(t)$, battery operation cost $C_{CBi}^{O}(t)$, and human resources cost $C_{HRi}(t)$.

$$\begin{aligned} C_{EVCSi}^{O}(t) &= C_{CHi}^{O}(t) + C_{EEi}^{O}(t) + C_{VCi}^{O}(t) + C_{CBi}^{O}(t) + C_{HRi}(t) \\ &= C_{pi}^{off}(t)P_{chi}^{N}T_{CHi} + C_{pi}^{off}(t)P_{EEi}^{max}T_{EEi} + C_{VCi}^{O}(t) \\ &\quad + C_{Bsi}^{O}(t)P_{ES} + C_{HRi}(t) \end{aligned} \tag{45}$$

where P_{chi}^{N} is the rated power of charging devices. T_{CHi} is the annual utilization hours of charging devices. P_{EEi}^{max} and T_{EEi} are the maximal power consumed and annual utilization hours of the electric devices respectively. $C_{Bsi}^{O}(t)$ is the operation cost of battery per unit and P_{ES} is capacity of battery.

The maintenance cost of charge station in the planning period can be express in Eq. (46).

$$C_{Evcsi}^{M}(t) = C_{ETi}^{M}(t)S_{ETi} + C_{CHi}^{M}(t)S_{CHi} + C_{DEi}^{M}(t)S_{DEi} + C_{BSi}^{M}P_{ES} \tag{46}$$

where $C_{ETi}^{M}(t)$, $C_{CHi}^{M}(t)$, C_{DEi}^{M} and C_{BSi}^{M} are the transformers, charging devices, other devices and batteries' battery per-unit capacity maintenance cost in ith charging station.

Network loss cost can be expressed in Eq. (47).

$$C_{PS}^{L}(t) = C_{Pi}^{on}(t)T_h P_{loss} \tag{47}$$

where $C_{Pi}^{on}(t)$ is the on-grid price of electricity. T_h is the annual utilization hour, and P_{loss} is the entire network loss.

(3) The yield per year for charge station can be express in Eq. (48).

$$Y_{EVCSi}(t) = \frac{\sum_{t=1}^{T} P_{EVCSi}(t)}{\left[\sum_{t=1}^{T} C_{EVCSi}^{T}(t)\right]T} \times 100\% \tag{48}$$

where $Y_{EVCSi}(t)$ is the average annual yield of charge station. T is the life time of charge station.

In order to mitigate the price inflation in 15 years the Net Present Value (NPV) is used

$$P_{Rt}(t) = P_{NPV} \times (1 + i)^t \tag{49}$$

where P_{Rt} is the net cash flow, P_{NPV} is the net present value, i is the discount rate, t is the time of cash flow.

Simulation results and discussions

The proposed method is applied to four different types of load profile in a test-line. The main aim is to demonstrate that the analytical method is suitable for identifying station two's locations under four different operation scenarios in terms of power loss reduction. The comparisons between two different methods illustrates in Table 5.

First scenario three different load profiles

For a uniformly distributed load, by comparing the objective function's values from Eq. (15) at each bus, bus 10 was obtained as the optimal location as the result of adding charge station two. By using the current density method the optimal location is $0.09l$ which is near bus 10. In this case both methods have the same result.

For the centrally distributed load, the optimal location x_0 is bus 8 using the analytical method. Whereas, by using current density method the optimal location x_0 is $0.22l$, which is near bus 9, not very accurate when compared with simulation results. Moreover, the non-optimal location can lead \$1210 of power loss than the optimal one.

For the increasing distributed load, the optimal location x_0 is bus 10, the bus 11 does not meet the design requirement as it can only provide energy to the load at bus 10. Whereas the current density method is $0.21l$, near bus 9. Compared with simulation results it is not accurate.

The Objective function's values and simulation results are shown in Figs. 8 and 9. By using the analytical method, the optimal location for charge station two for both uniformly load and increasingly load type profiles are bus 10. For centrally load is bus 8. Simulation results prove analytical approach.

Second scenario three different load profiles

For the second scenario P_{dis1} and Q_{dis1} is optimised. $P_{dis2} = 0$, $Q_{dis2} = 0$, $P_{char2} = P_{dis1}$, $P_{optimal} = P_{dis1}$. Different optimised active and reactive power of charge station one are shown in Table 6. They are used as input data of Eq. (15).

The objective function's values for three types of load profile show in Fig. 10.

The simulation results demonstrate the analytical approach, bus 11 in this scenario does not meet the design requirements which cannot provide the energy to the load nearby. Therefore, bus 3 is chosen for three types of load.

Third scenario three different load type

For the third scenario, P_{dis2} and Q_{dis2} is optimised. $P_{dis1} = 0$, $Q_{dis1} = 0$, $P_{char1} = P_{dis2}$, $P_{optimal} = P_{dis2}$. Differently optimised active and reactive power of charge station two shows in Table 7.

The objective function's values meet the simulation results in this scenario for three different types of load profile. The optimal location for uniformly load type is bus 7, for centrally load type is bus 5, for increasingly load type is bus 8. The simulation results prove the analytical method (see Fig. 11).

Fourth scenario three different load profiles

For the fourth scenario, $P_{dis1} = 0$, $Q_{dis1} = 0$, $P_{dis2} = 0$, $Q_{dis2} = 0$. Active and reactive power from grid are optimised and obtained by using the MATLAB optimisation programming. Table 8 shows the different active and reactive power from the TN for uniformly load.

For this scenario, both charge stations are regarded as the loads. The charge station one is added into bus 2, charge station two is added to the flowing bus except bus 2. The differently optimised active and reactive power from TN are set as the input data of Eq. (15) (see Fig. 12).

Regarding the first scenario, for the uniformly load and increasingly load, the station two's location is bus 10 and it is relatively far from bus one's location. Therefore, the power loss caused by the edge of test line is much smaller than the one installed in the middle. For the centrally load the station two location moves a little closer to the centre because of the load type.

Table 5
The comparisons between two methods for the first scenario centrally load.

Method	Power loss expressions	Location expression	Location	Simulation results	Power loss (\$)
Current density	$P_{loss}(T_i) = \int_0^l dP(x, T_i)$	$\frac{\overline{P_{loss}}(x_0)}{d_{x_0}} = 0$	0.22*l* (Bus9)	Bus 8	\$12,902
P, *Q* dispatch	$P_{loss}(T_i) = \sum_{\forall s_1, s_2}^{s_1, s_2 \in S_8} \left(\frac{P_{s_1}^2 + Q_{s_1}^2}{V_{s_1}^2}\right) R_i$	$Min\ f_j = \sum_{i=1}^{j} R_{1i(j)} \lvert P_i' + jQ_i' \rvert^2, \quad j = 3, 4, 5 \cdots N$	Bus 8	Bus 8	\$11,692

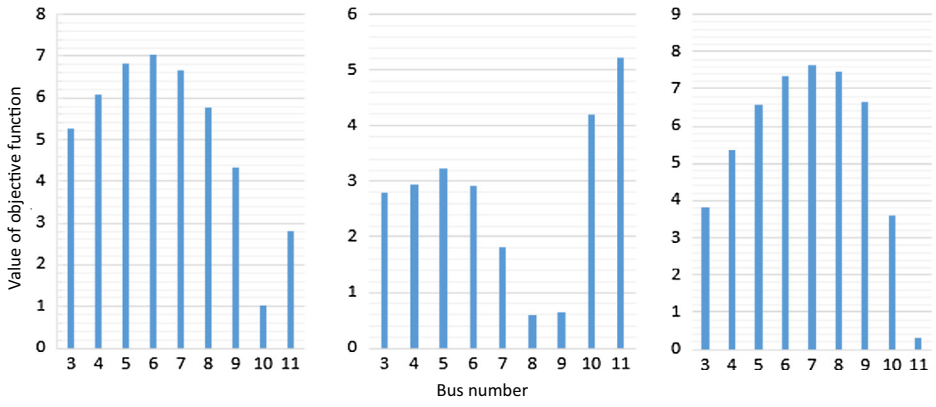

Fig. 8. Objective function's values of the first scenario of three load profiles.

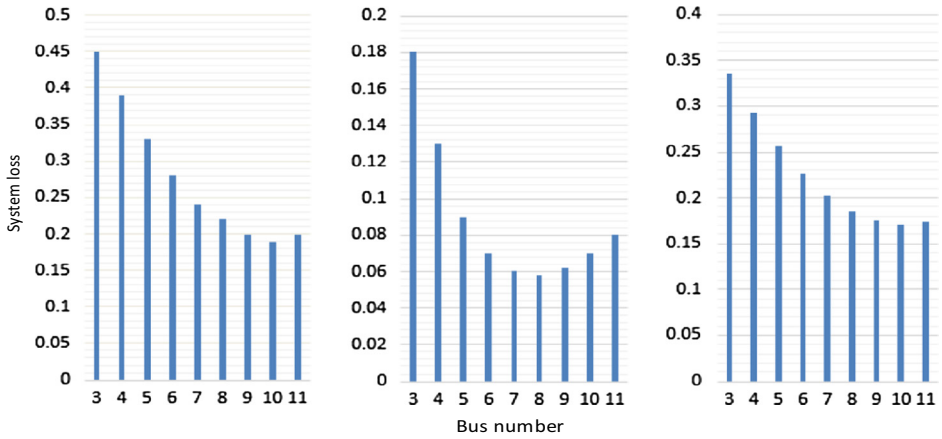

Fig. 9. Simulation results of the first scenario of three load.

Table 6
P, *Q* station one at different locations for uniformly load.

P, *Q*	No.								
	3	4	5	6	7	8	9	10	11
P_{dis}	3.88	3.84	3.80	3.58	3.25	2.69	2.08	1.47	1.15
Q_{dis}	1.25	1.37	1.61	1.21	1.05	0.93	0.62	0.48	0.27

For the second scenario, station one needs to transfer energy to station two. For all three types of load the location of station two is bus 3, because in this situation station two was regarded as the largest load and cannot provide any energy to the loads. Therefore, the optimal locations for all three types of load is bus 3.

For the third scenario, charge station two needs to deliver energy to station one. For uniformly load type, station two location is bus 7. Because bus 7 is in the middle area of test line, it is not far from station one and the load at the edge. For the centrally load type the location is bus 5, which is in the centre of the test line, near to the largest load bus 6 and the second largest load bus 2. For increasingly load type the location is bus 8. For this load type, if station two is installed at the end of the test line the power loss will increase during the energy transmission to station one. Hence, bus 8 is the ideal location.

With regard to the fourth scenario. When both charge stations run out of rated energy, charge station two's location is bus 3 for three different loads. Because for uniformly load and centrally load, bus 2 and 3 are the largest load bus. Meanwhile, bus 3 is the nearest bus to the transmission network, so that the network does not need deliver as much power to bus 3 as to others. For increasingly load, although the largest load is bus 10 when the station is seen as load and added into that bus. Bus 3 is the second largest load of the system, and only less than the largest load bus 10, 0.87 MW. Bus 10 is at nearly the end of this test line so that much more energy needs to be transferred to that bus. Therefore, for this scenario the location for station two is bus 3.

Discussion

Table 9 shows the optimal locations for charge station two in the test-line for power loss reduction. From the system operating view point, four different operation scenarios have different station two's locations. They give system operators suggestions for power loss reduction operations. However in reality, there is low possibility for moving station two's locations along the test-line according to different operation scenarios, unless every bus has charge stations. Yet it is expensive to install them in every bus. Therefore, from system planning view point, for each load type of four operation scenarios, charge station two's locations should be fixed.

As mentioned above, the method to identify fixed charge station two's locations show below.

In most operation states, charge stations work under the first scenario. Therefore, a compromise is made, if the station two's

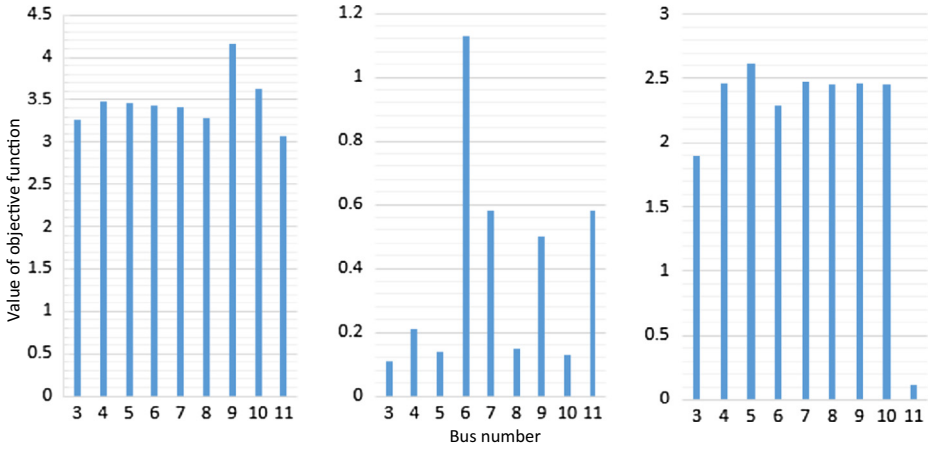

Fig. 10. Objective function's values for the second scenario of three load profiles.

Table 7
P, *Q* station two at different locations for uniformly load.

P, *Q*	No.								
	3	4	5	6	7	8	9	10	11
P_{dis}	3.81	3.79	3.77	3.63	3.20	2.68	2.03	1.09	0.58
Q_{dis}	1.47	1.50	1.56	1.29	1.19	0.93	0.61	0.48	0.27

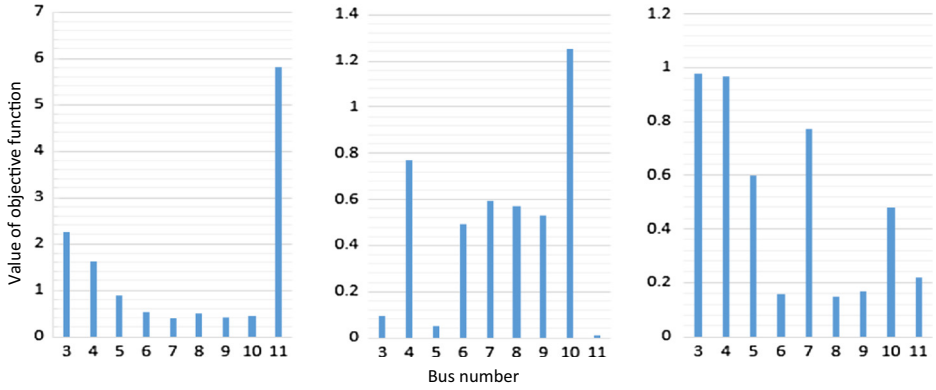

Fig. 11. Objective function's values for the third scenario of three load profiles.

Table 8
P_{grid}, Q_{grid} from TN at different locations for uniformly load.

P, *Q*	No.								
	3	4	5	6	7	8	9	10	11
P_{dis}	9.45	9.51	9.56	9.62	9.67	9.72	9.77	9.83	9.85
Q_{dis}	2.95	3.00	3.04	3.09	3.14	3.18	3.22	3.25	3.27

locations in the second scenario and the third scenario can be changed to the first scenario's locations, the fixed station two's locations can be obtained. In order to observe the differences in terms of active–reactive power loss. When changing the third and second to the first scenario, and to analyse the possibilities of swapping station two's locations. The increasingly load type for the second and the third scenario is chosen as a case study.

When station two moves from bus 3 to bus 10 for the second scenario, and moves from bus 8 to bus 10 for the third scenario. As can be seen from Table 10, station two moves from bus 3 to bus 10 the test-line's power loss increases much for the second scenario. However, for the third scenario, active and reactive power loss do not increase dramatically when changing charge station two's location from bus 8 to bus 10. Therefore, if charge station two can move from bus 8 to 10 rather than from bus 3 to 10, 0.319 MW power loss can be saved.

Based on above analysis, an assumption is made that charge station one should always run out of energy before station two. Meaning that the third scenario always occurs before the second scenario. For the sake of implementing it, charge station two's capacity has to be increased, whereas station one's capacity needs to be decreased.

The capacity of station two rises a little by $\frac{4}{3}$ of original capacity and station one's capacity declines by $\frac{2}{3}$ of original capacity.

From Table 11 the current parameters of both stations are used for an increasingly load type for the first, and the third scenario.

Table 12 shows charge station two's locations of new capacity for both stations of the power loss. Although, the rated power of station two increased to 1.36 MW, and station one decreased to 0.68 MW, the optimal location for station two is still bus 10. Table 12 indicates charge station two's active and reactive power of new capacity. Using the changed capacity of both stations in the third scenario of increasingly load type, the optimal location for station two is still bus 8. Also from Table 13, if station two's

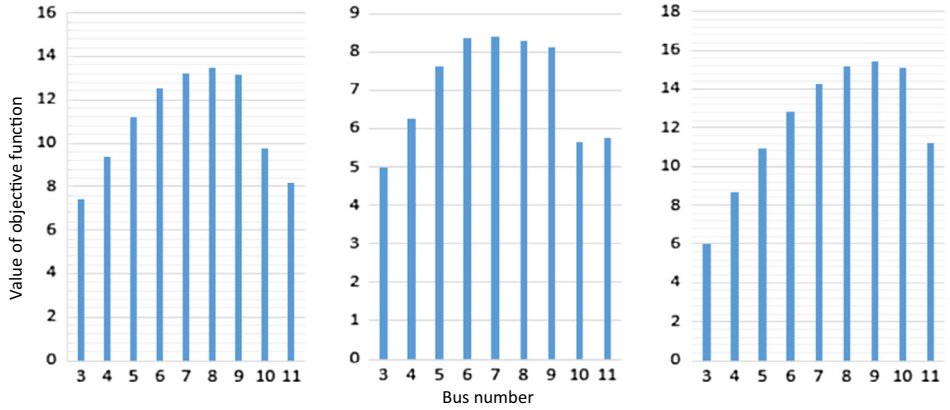

Fig. 12. Objective function's values for the fourth scenario of three load types.

Table 9
The optimal location of charge station two.

Different scenarios	Uniformly load	Centrally load	Increasingly load
First scenario	Bus NO. 10	Bus NO. 8	Bus NO. 10
Second scenario	Bus NO. 3	Bus NO. 3	Bus NO. 3
Third scenario	Bus NO. 7	Bus NO. 5	Bus NO. 8
Fourth scenario	Bus NO. 3	Bus NO. 3	Bus NO. 3

Table 10
Power loss difference for increasingly load type.

	For the second scenario			For the third scenario		
Bus NO.	3	10	Difference	8	10	Difference
P_{loss}	0.387	0.741	0.354	0.094	0.129	0.035
Q_{loss}	0.33	0.64	0.31	0.08	0.11	0.03

Table 11
BESS related parameters.

Stations	Original		Current	
	Power	Capacity	Power	Capacity
Station one	1.02 MW	4.08 MW h	0.68 MW	2.72 MW h
Station two	1.02 MW	4.08 MW h	1.36 MW	5.44 MW h

Table 12
Charge station two's locations for increasingly load of first scenario of new capacity.

P, Q	No.								
	3	4	5	6	7	8	9	10	11
P_{loss}	0.48	0.42	0.34	0.32	0.29	0.26	0.24	0.23	0.24
Q_{loss}	0.42	0.36	0.32	0.28	0.25	0.25	0.21	0.21	0.21

Table 13
P, Q and power loss for the third scenario of increasingly load.

P, Q	No.								
	3	4	5	6	7	8	9	10	11
P_{disc}	4.58	4.80	4.37	3.75	3.55	2.99	2.57	2.20	1.15
Q_{dis}	2.13	2.26	1.85	1.34	1.23	0.85	0.62	0.48	0.27
P_{loss}	0.35	0.26	0.19	0.14	0.10	0.095	0.10	0.12	0.28
Q_{loss}	0.30	0.22	0.16	0.12	0.09	0.08	0.09	0.10	0.24

locations change to bus 10, the active and reactive power loss will not change significantly compared with other changes. Therefore, replacing station two's location from bus 8 to bus 10 can be applied in the test-line from a system planning point view.

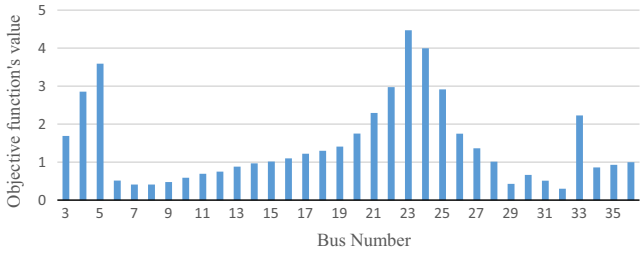

Fig. 14. Objective function's values of 36-bus test distribution network.

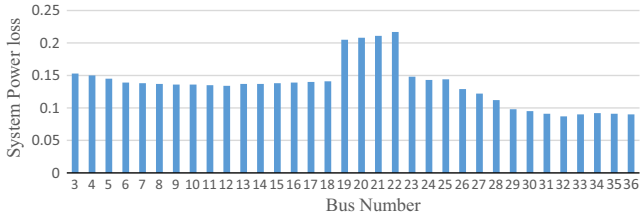

Fig. 15. The power loss of the 36-bus test distribution network.

Fig. 16. The revenue, cost, profit of charge station in every 5 year.

The proposed method was also tested in a 36-bus distribution networks [32]. The simulation results prove the accuracy of the proposed method. The objective function values and the simulation results can be seen in Figs. 14 and 15.

The objective function values were obtained by using the already proposed method and are shown in Fig. 13. It can be seen that the optimal location for charging station two in terms of power loss reduction is bus 32, the lowest objective function value in Fig. 14. From the simulation results in Fig. 15, it can be seen that the proposed method is accurate, installing charging station two at bus 32 leads the system to have the lowest power loss.

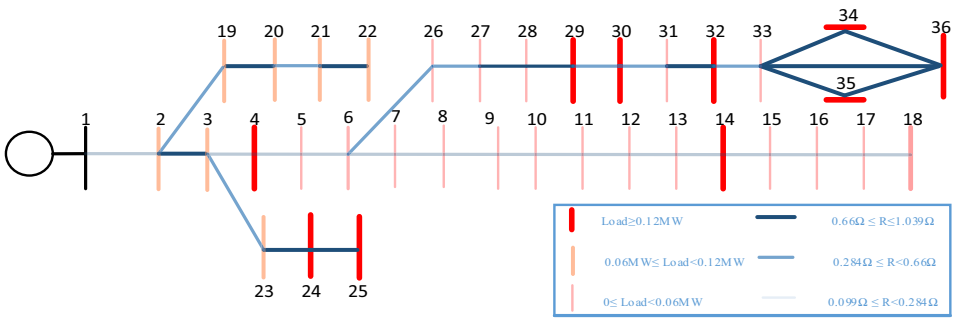

Fig. 13. The topology of 36-bus distribution network.

Fig. 16 shows commercial aspects of charge stations. The blue[1] one is 5 years revenue, the red one is cost and the grey one is profit. As we can see from Fig. 16 in the first 5 years, station owners need to invest charging facilities that makes negative profits. However, in the after 5 years state owners can not only repay the investment cost, but 0.23 million profit can be taken by selling the cheaper electricity to local residents and EVs. In the 15 years the station owners can obtain 0.84 million profits. These profits can be obtained from Eqs. (39) and (49).

Overall, from above analysis due to choosing the fixed locations of station two. Comparisons are made for replacing station two' locations from bus 3 and 8 to bus 10 and, the result of moving station two from bus 8 to bus 10 is more suitable than 3 to 10. In order to apply this, the capacities of station one changed to 2.72 MW h, and station two's capacity changed to 5.44 MW h making scenario three always occurs before scenario two.

As a result of swapping station two's location from bus 8 to bus 10, the difference of active and reactive power loss only changes 0.025 MW and 0.02 Mvar. Therefore, bus 10 can be used instead of other buses for installing station two for power loss reduction both from system operation and planning points of view. All the results are obtained from MATPOWER and MATLAB optimisation programming.

Conclusion

In this paper, we used a new analytical analysis combined with active and reactive power optimisation methods for identifying charge station two's best location in terms of power loss reduction. The method was tested in an 11-bus distribution line. While, a previously developed current density method [14] is used and the results are compared for the same test-line, with four different operational scenarios for power loss reduction. In addition, the proposed method was tested in a 36-bus distribution network, the simulation results prove the accuracy of the method for more complicated networks.

As a results it was shown that 27% of average active power loss can be saved by installing two charge stations rather than no charge stations. From the power flow analysis, it was proved that the current density method is not accurate for choosing charge stations two's location. Based on four different operation scenarios, 17% of average active power loss can be saved for three different types of load, using the new method described in this paper compare with current density method, and the average annual yield above inflation is 2.6%, which can be refer to Eq. (48) for the station owners.

References

[1] Tang X, Lv L, Liu Y, Xiang Y, Zhang L. Researches on electric vehicles access in demonstration district considering network losses. In: Power and energy engineering conference (APPEEC), 2012 Asia-Pacific, Shanghai. p. 1–6.

[2] bdelhamid Singh MA, Singh R, Qattawi A, Omar M, Haque I. Evaluation of on-board photovoltaic modules options for electric vehicles. IEEE J Photovolt 2014;4(6):1576–84. http://dx.doi.org/10.1109/APPEEC.2012.6307220.

[3] Singh M, Kumar P, Kar I. Designing a multi charge station for electric vehicles and its utilization for the grid support. In: Power and energy society general meeting, 22–26 July, 2012 IEEE. p. 1–8.

[4] Ota Y, Taniguchi H, Nakajima T, Liyanage KM, Baba J, Yokoyama A. Autonomous distributed V2G (vehicle-to-grid) satisfying scheduled charge. IEEE Trans Smart Grid 2011(99):1–6.

[5] Timpner J, Wolf L. Design and evaluation of charge station scheduling strategies for electric vehicles. IEEE Trans Intell Transp Syst 2014;15(2):579–88.

[6] Xu F, Yu GQ, Gu LF, Zhang H. Tentative analysis of layout of electrical vehicle charge stations. East China Electr Power 2009;37:1678–82.

[7] Liu ZF, Zhang W, Ji X, Li K. Optimal planning of charge station for electric vehicle based on particle swarm optimization. In: Innovative smart grid technologies – Asia (ISGT Asia), IEEE, 21–24 May, 2012. p. 1–5.

[8] Yao Weifeng, Zhao Junhua, Wen Fushuan, Dong ZhaoYang, Xue Yusheng, Xu Yan, et al. A multi-objective collaborative planning strategy for integrated power distribution and electric vehicle charging systems. IEEE Trans Power Syst 2014;29(4):1811–21.

[9] Li Y, Li L, Yong J, Yao Y, Li Z. Layout planning of electrical vehicle charge stations based on genetic algorithm. In: Electrical power systems and computers. Lecture notes in electrical engineering, 1, vol. 99. p. 661–8.

[10] Ge S, Feng L, Liu H. The planning of electric vehicle charge station based on grid partition method. In: IEEE electrical and control engineering conference, Yichang, China.

[11] Machiels N, Leemput N, Geth F, Van Roy J, Buscher J, Driesen J. Design criteria for electric vehicle fast charge infrastructure based on flemish mobility behavior. IEEE Trans Smart Grid 2014;5(1):320–7.

[12] Cairo J, Sumper A. Requirements for EV charge stations with photovoltaic generation and storage. In: 3rd IEEE PES international conference and exhibition on innovative smart grid technologies (ISGT Europe), 14–17 October, 2012. p. 1–6.

[13] Ding Huajie, Hu Zechun, Song Yonghua, Hu Xiaorui, Liu Yongxiang. Coordinated control strategy of energy storage system with electric vehicle charging station. In: IEEE conference and expo on transportation electrification Asia-Pacific (ITEC Asia-Pacific), August 31, 2014–September 3, 2014. p. 1–5.

[14] Atwa YM, El-Saadany EF. Optimal allocation of ESS in distribution systems with a high penetration of wind energy. IEEE Trans Power Syst 2010;25(4):1815–22.

[15] Carpinelli G, Mottola F, Proto D, Russo A. Optimal allocation of dispersed generators, capacitors and distributed energy storage system sin distribution networks. Modern Electr Power Syst 2010:1–6.

[16] Celli G, Mocci S, Pilo F, Loddo M. Optimal integration of energy storage in distribution networks. IEEE Power Tech 2009:1–7.

[17] Du Y, Yun BF. Optimal allocation of energy storage system in distribution systems. Adv Control Eng Inform Sci 2011;15:346–51.

[18] Wang CS, Nehrir MH. Analytical approaches for optimal placement of distributed generation sources in power systems. Power engineering society general meeting, IEEE, 12–16, vol. 3. p. 2393.

[19] Owen P. Powering the nation household electricity-using habits revealed. London: Energy Saving Trust; 2011. EST.Rep..

[20] Miller NW, Zrebiec RS, Hunt G, Deimerico RW. Design and commissioning of a 5 MVA, 2.5 MW h battery energy storage system. In: Proc IEEE transaction distribution conf, Los Angeles, August 2007. p. 339–45.

[21] Voeclcker J. GreenCarreportWebpage; 2012. <http://www.greencarreporrts.com/news/1078116_july-plug-in-electric-car-sales-volt-steady-leaflethargic-again>.

[22] Voelcker J. GreenCarReportsWebpage; 2012. <http://www.greencarreports.com/news/1081419plug-in-electric-car-sales-tripleiin2013-as-buyers-models-increase>.

[23] Cole J. GreenCarReport.Webpage; 2013. <http://insideevs.com/september-2013-plug-in-electric-vehicle-sales-report-card/>.

[24] OxfordshireCountyCouncil; 2016. Electric avenues: Oxford set to install 100 electric vehicle charging stations in residential streets. <https://www.oxfordshire.gov.uk/cms/news/2016/jan/electric-avenues-oxford-set-install-100-electric-vehicle-charging-stations-residential>.

[25] Alternative Fuels Data Center. Developing infrastructure to charge plug-in electric vehicles. <http://www.afdc.energy.gov/fuels/electricity_infrastructure.html>.

[26] Jin Chenrui, Tang Jian, Ghosh P. Optimizing electric vehicle charging with energy storage in the electricity market. IEEE Trans Smart Grid 2013;4(1):311–20.

[27] Walker LH. 10-MW GTO converter for battery peaking service. IEEE Trans Ind Appl 1990;26(1):63–72.

[28] Gabash A, Li P. Active–reactive optimal power flow in distribution networks with embedded generation and battery storage. IEEE Trans Power Syst 2012;27(4):2026–35.

[29] Gabash A, Li P. Evaluation of reactive power capability by optimal control of wind-vanadium redox battery stations in electricity market. Renew Energy Power Qual J 2011;9:1–6.

[30] Nail SG, Khatod DK, Sharma MP. Optimal allocation of combined DG and capacitor for real power loss minimization in distribution networks. Electr Power Energy Syst 2013;53:967–73.

[31] Liu Zhipeng, Wen Fushuan, Ledwich G. Optimal planning of electric-vehicle charging stations in distribution systems. IEEE Trans Power Deliv 2013;28(1):102–10.

[32] Su Ching-Tzong, Lin Chen-Yi, Wong Ji-Jen. Optimal size and location of capacitors placed on a distribution system. WSEAS Trans Power Syst 2008;3(4):247–56.

[1] For interpretation of colour in Fig. 16, the reader is referred to the web version of this article.